Development of an optical biochip for the analysis of cell environment sensitivity

David Morris[1], Andrew Goater[1,2], Anoop Menachery[1], Julian Burt[1], Nadeem Rizvi[2], Daniel Matthews[3], Huw Summers[3], Iestyn Pope[4], Boris Vojnovic[4], Kerenza Njoh[5], Sally Chappell[5], Rachel Errington[5], Paul Smith[5].

[1]School of Electronic Engineering, University of Wales, Bangor, Dean Street, Bangor, Gwynedd LL57 1UT, United Kingdom

[2]UK Laser Micromachining Centre, Dean Street, Bangor, Gwynedd LL57 1UT, United Kingdom

[3]School of Physics and Astronomy, Cardiff University, The Parade, Cardiff CF24 3YB, United Kingdom

[4]Gray Cancer Institute, University of Oxford, Oxford, United Kingdom

[5]School of Medicine, Cardiff University, Heath Park, Cardiff, CF14 4XN, United Kingdom

ABSTRACT

An optical biochip is being developed for monitoring the sensitivity of biological cells to a range of environmental changes. Such changes may include external factors such as temperature but can include changes within the suspending media of the cell. The ability to measure such sensitivity has a broad application base including environmental monitoring, toxicity evaluation and drug discovery. The device under development, capable of operating with both suspension and adherent cell populations, employs electrokinetic processes to monitor subtle changes in the physico-chemical properties of cells as environmental parameters are varied. As such, the device is required to maintain cells in a viable condition for extended periods of time.

The final device will employ integrated optical illumination of cells using red emitting LED or laser devices with light delivery to measurement regions achieved using integrated micro-optical components. Measurements of electrokinetic phenomena such as dielectrophoresis and electrorotation will be achieved through integrated optical detectors. Environmental parameters can be varied while cells are actively retained within a measurement structure. This enables the properties and sensitivity of a cell population to be temporally tracked.

The optical biochip described here uses a combination of microfabrication techniques including photolithographic and laser micromachining processes. Here we describe the design and manufacturing processes to create the components of the environmental monitoring strutures of the optical biochip.

Keywords: Optical Biochip, Electrokinetics, Microfabrication, Laser Micromachining.

INTRODUCTION

Biochips bring together the accuracy and flexibility of microfabrication processes with biological or chemical assays to create an integrated environment for biotechnological processing. The potential of biochip technology extends over a wide range of market sectors dominated by the benefits in healthcare and drug discovery but also including sectors such as food and environmental monitoring and analysis. Optical biochips extend the fundamental biochip concept to include optical principles either as part of a monitoring process such as absorbance or fluorescence measurement or as an

essential part of a reaction chain or assay such as photosynthesis and similar processes. Optical biochips can make use of external or integrated light sources and detectors but typically contain integrated optical delivery components such as light or waveguides, reflectors and lenses. While there are many examples of optical integration within biochip devices, the development challenges in optical biochips are moving towards the integration of optical systems typically associated with complex optical bench configurations and high costs. To meet such challenges advances in biotechnology for assay formatting, physics and electronics for optical component development and microfabrication are required.

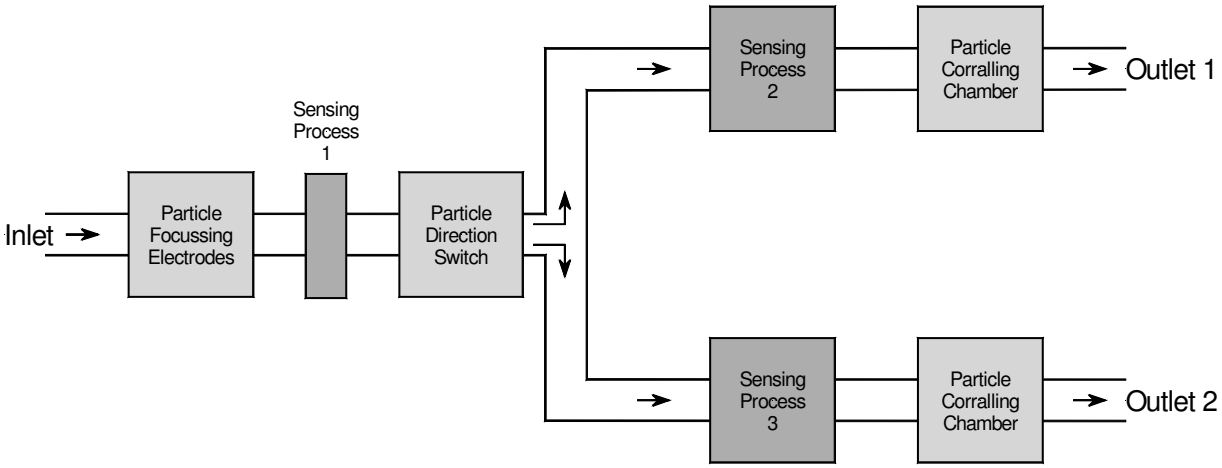

Fig. 1 Conceptual diagram of a simple optical biochip for biological cell analysis and subsequent separation

Figure 1 shows a conceptual diagram of a simple optical biochip for the analysis and subsequent separation of a mixed population of biological cells. The diagram divides the key processing steps into unit blocks. Several different technologies can be used in each block. For instance, in this work, the particle direction switch on the main inlet channel is an electrokinetic module which uses microelectrode generated electric fields to direct cells within the sample along either outlet branch. However, such direction switching could be implemented using mechanical valves, additional fluid flows or even magnetic beads if the cells are selectively labeled with magnetic particles. The device outlined in figure 1 analyses a mixed population of cells which are introduced through the inlet channel. Cells are focused into a narrow stream at a defined lateral position within the channel. This stream corresponds to the optimum position of an optical sensor which detects a specified sub population of cells within the channel. Knowledge of the cell velocity allows the switching unit to direct cells within the detected sub population along one outlet branch while other cells are directed along the second outlet branch. Within these branches, secondary sensing units can undertake further analysis of the cell population while corralling chambers can be used to collect and hold further sub populations identified in the secondary sensing processes. It is the development of these corralling chambers that is discussed here.

In many areas of biotechnology there is a need to be able to assess the reaction of single cells or cell populations to changes in their physical or chemical environment. An example of a study of response to a change in physical environment could be the monitoring of the generation of heat shock proteins by cells as environmental temperature is changed. Chemical changes to an environment could include the evaluation of potential drug toxicity to a particular cell type. For adherent cell lines changes in cell environment can easily be introduced since cells become attached to surfaces within the biochip. Changes such as temperature can be applied to defined locations whereas chemical changes can be introduced by the flow of a suitable media over the attached cells. For suspension cells, environmental changes on a defined group of cells are less easy to implement. Often the cells are required to be maintained in suspension with a continuous fresh supply of medium if cells are to be studied over prolonged periods. Here we describe the use of microfluidic vortex-like structures combined with optional electrokinetic forces to hold cells within a continuously moving fluid flow.

1 MICROFLUIDIC DESIGN

1.1. Overview

Within the optical biochip shown in figure 1 cell corralling and collection occurs in a containment chamber located adjoining the main fluidic outlet channel. The chamber is circular is nature with an opening onto the main outlet channel and a narrow control channel opposite the opening. Cells can be directed into and out of the chamber by a number of means. The simplest method for directing cells into the chamber is to restrict the fluid flow through the outlet channel and direct all flow through the control channel. Alternatively, electrokinetic forces can be used to direct cells across the inlet side of the media channel and selectively 'push' cells into the containment chamber. Once cells are within the chamber, closing the control channel allows cells to be held within the containment chamber. Allowing a fluid to flow along the media channel, past the entrance to the containment chamber, causes the fluid within the containment chamber to move and circulate [1]. While a small portion of the fluid within the chamber will flow into the media channel, this is balanced by fresh media entering from the media channel into the containment chamber. At the same time, chemical species in the circulating fluid within the containment chamber diffuse into the fluid stream within the media channel and vice versa. Cells within the containment chamber are carried by the fluid flow and circulate around the chamber so keeping the cells in suspension. To prevent loss of cells optimal chamber design is required. Further control of cell position can be achieved using AC electrokinetic forces to 'push' cells towards the rear of the chamber as they circulate. Figure 2a shows a schematic diagram of the containment chamber including a series of optional microelectrodes which can be fabricated on either or both the upper and lower surfaces of the containment chamber. The electrodes can be used to both generate AC electrokinetic forces or to sense changes within the chamber fluid composition. In this work cell characteristics were detected by monitoring the dielectrophoretic collection of cells onto microelectrodes photolithographically fabricated on the lower surface of the chamber.

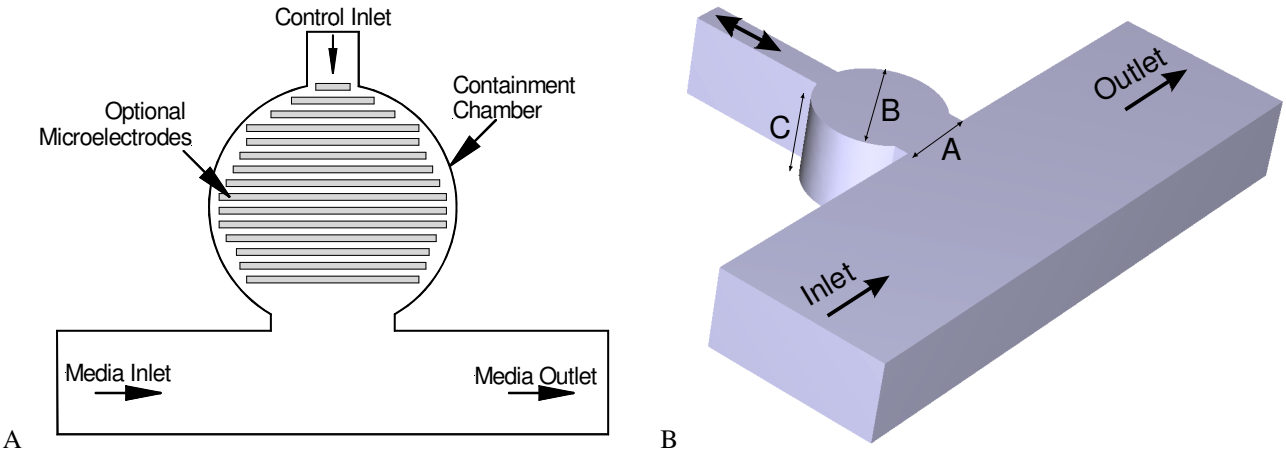

Fig. 2 (A) Outline diagram of the cell containment chamber illustrating operational components. (B) 3D view of the fluidic chamber showing dimensions that significantly influence the fluid flow profiles within the chamber.

1.2. Simulation

Figure 2b shows a 3D representation of the containment chamber and identifies three critical dimensions which, in combination, determine the nature of the fluid flow within the containment chamber. The dimensions of the main media channel effectively control the velocity of the fluid at the chamber entrance. Since laminar flow regimes exist within the media channel the fluid velocity across the chamber entrance is significantly lower than the fluid velocity at the centre of the channel.

Finite element analysis was used understand and optimize the operation of the containment channel. All modeling work was carried out using Comsol Multiphysics 3.3 (Comsol AB, Sweden) to generate a multiphysics model to combine fluid flow analysis with chemical diffusion, forced convection and electrical field analysis within a conductive media.

1.2.1. Microfluidic Flow

Fluid flow was simulated by the finite element solution of the incompressible form of the Navier-Stokes equation. Chamber models of the form of figure 2b were generated with varying chamber entrance width, chamber height and chamber diameter. Depending on these dimensions, the simulation model comprised of between 30,000 and 40,000 degrees of freedom. The models assumed that aqueous media flowed from the media inlet towards the media outlet with the control channel having a blind termination away from the containment chamber. Parabolic entrance flow was defined at the media inlet with a defined peak fluid velocity. The distance between the inlet and entrance of the containment chamber was sufficient run in to allow the simulation software to calculate the true flow profile before the entrance of the containment chamber. Figure 3 shows the fluid velocity vectors for a 400µm high, 620µm diameter chamber with a 400µm wide entrance. The vectors clearly show the circulatory nature of the fluid flow with the velocity on the entrance side significantly larger than the control channel side of the chamber.

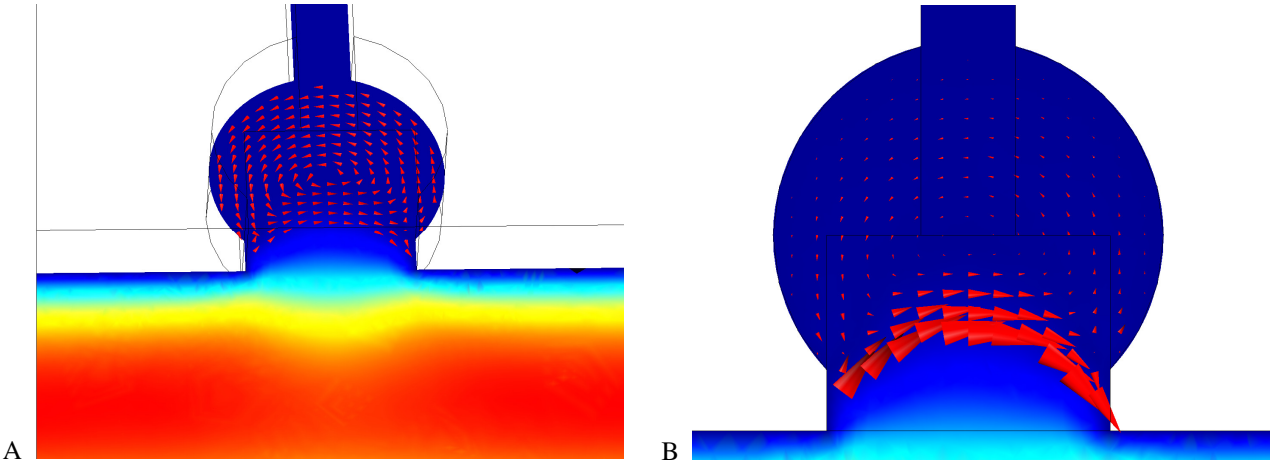

Fig. 3 Fluid flow profiles within a 400µm high, 620µm diameter optical biochip containment chamber with a 400µm wide entrance. (A) Normalized fluid flow vectors showing the circulatory nature of the fluid flow within the chamber. The parabolic laminar flow profile within the media channel is shown by shading levels in the lower part of the image. (B) Proportional fluid flow vectors showing higher velocity past the chamber entrance compared to the rear of the chamber.

The vortex nature of the fluid flow in the chamber can be optimized by varying the relative dimensions of the chamber height, diameter and entrance width. Figure 4 shows the influence these parameters have on the vortex operation. Figure 4a shows the position of the vortex centre within the chamber. Vortex formation was not possible for entrance aperture widths greater than the data shown for each chamber height. Figure 4b shows the influence of the entrance aperture area on the maximum velocity at the chamber entrance. The greater the aperture the more the media channel fluid flow encroaches into the containment chamber. Figure 4c shown the maximum velocity of the vortexing fluid in the opposite direction to the, driving, media channel fluid flow. These simulation measurements were taken at the mid height of the containment chamber. The graphs of figure 4 show that there is an optimum combination of dimensions for the formation of vortex flow within the containment chamber. Vortexing will only occur for a defined range of entrance aperture areas with the maximum vortex velocity being determined by the aspect ratio of the entrance aperture. Maximum vortex velocity occurs when the entrance width to chamber height ratio is of the order of 0.8.

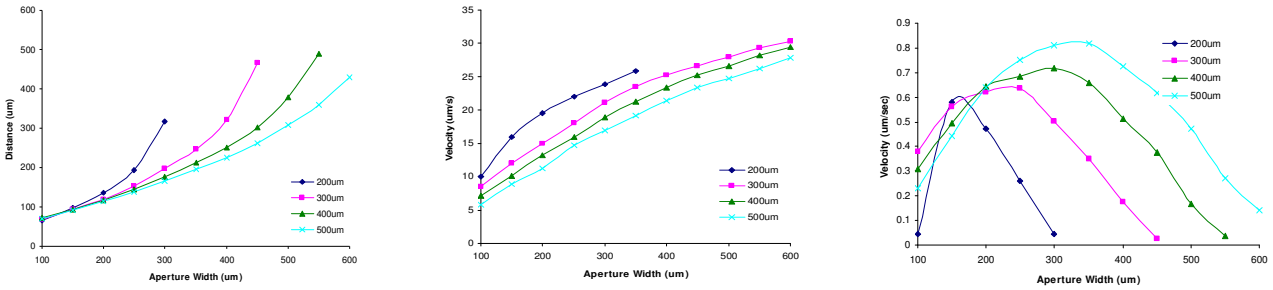

A B C

Fig. 4 The influence of chamber height and entrance aperture width on the fluid flow within a 620µm diameter containment chamber. (A) The variation in the position of the vortex centre from the middle of the chamber entrance measured perpendicular to the media channel. (B) Variation in fluid velocity at the centre of the chamber entrance aperture. (C) Maximum fluid vortex velocity in the opposite direction to the media channel fluid flow.

1.2.2. Diffusion and convection

Changing the chemical environment within the containment chamber is achieved by altering the composition of the fluid flowing along the media channel. Changes in the composition of the containment chamber fluid occur as a result of forced convection and diffusion processes between the chamber fluid and the media channel fluid. Typically cells are suspended in ionic media roughly equivalent to a sodium chloride concentration of 150mM. For this work the containment chamber was used to demonstrate the sensitivity cell electrokinetic motion to variations in the electrical conductivity of their suspending medium. To this end, the variation in the concentration of sodium and chloride ions within the containment chamber was simulated. The initial conditions for the simulation defined the concentration of both species in the containment chamber to be 150mM while the concentration within the media channel was set to zero. Figure 5a shows the variation in average vortex chamber sodium chloride concentration with time for a media channel fluid with a peak flow velocity of 100µm/s. It can be seen that at this low flow velocity a 50x reduction in conductivity is achieved in 15 minutes.

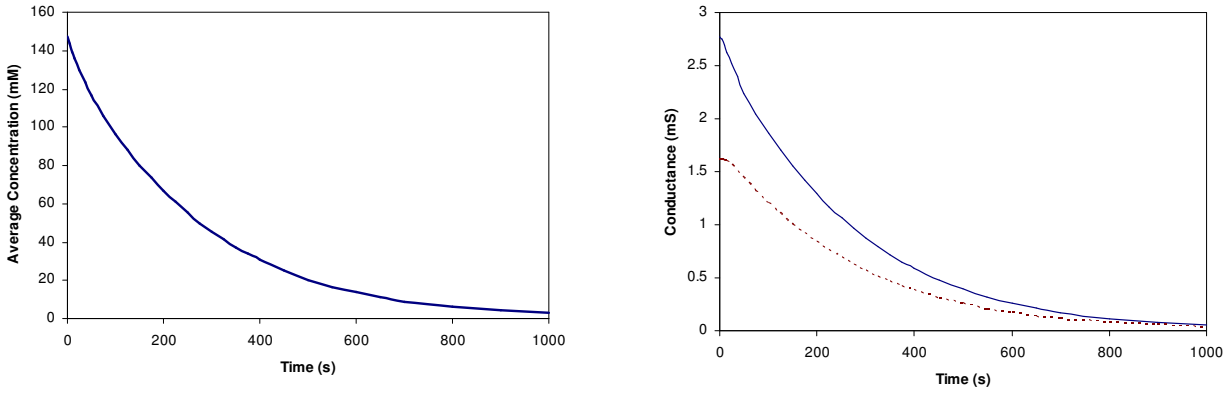

A B

Fig. 5 (A) Graph of the simulated average sodium chloride concentration within the sample chamber with time for a media channel peak velocity of 100µm/s. (B) Graph of simulated measured conductance for all electrodes shown in figure 2a (solid) and rear half of the electrodes in figure 2a (dashed)

1.2.3. Electrical conductivity

The electrodes shown in figure 2a can be used for both the generation of AC electrokinetic forces to assist in the retention of cells in the vortex flow or for sensing changes in electrical conductance within the chamber resulting from

changes in the chemical composition of the chamber fluid. Simulation of this sensing application is shown in figure 5b. The solid line represents the measured conductance using all electrodes in figure 2a while the dashed line shows the conductance measured using the 8 electrodes positioned furthest from the chamber entrance. In both cases the electrodes were energized with alternate positive and negative equal voltages so causing conductance measurements to be dominated by the conductivity of chamber media between adjacent electrodes. Both graphs show a high initial conductance which drops rapidly as the chamber conductivity is reduced. The initial measured conductance is a function of the effective areas of the two electrode groups. The difference in the rate of conductance reduction is influenced by the fact that when all electrodes are used, there is a significant area of the electrodes that is measuring the fluid from the media channel as it encroaches into the chamber entrance. Since this fluid is designated to have zero sodium chloride concentration it will cause these electrodes to measure a conductance close to zero and so give a steeper initial reduction. Both electrodes approach the same conductance after 15mins when the chamber fluid concentration gradient is less.

2 DEVICE FABRICATION

Simulation studies of the containment chamber performance led to critical chamber dimensions of 720µm diameter, 320µm height and an entrance width of 360µm. A simple chamber containing biochip was designed and fabricated to fit into a microfluidic platform consisting of a Perspex base plate into which a series of fluid delivery and extraction pipes had been machined. The pipes led to a series of regularly spaced openings which mated, using small rubber o-rings, to the underside of the biochip device. Good fluid seals between the platform and biochip were ensured by clamping an upper Perspex plate over the biochip. The upper plate contained a 2.5cm diameter circular beveled hole to allow microscope observation of cells within the biochip chamber.

Laser micromachining was used to create the fluidic components of the biochip. Laser micromachining as a manufacturing technique has emerged from the development of micro and nanotechnologies over the past two decades. While laser micromachining is still considered a new process in many areas of microengineering, it has become an established manufacturing method in niche application areas such as inkjet printer nozzle drilling [2] and flat panel display patterning [3]. Accurate laser micromachining tends to use pulsed lasers at wavelengths and pulse durations where heating and melting based surface disruption is minimal. By controlling the number of laser pulses, and hence the total incident radiation, precise machining depths can be achieved while minimal thermal distortion occurs. In this work a femtosecond pulsed infrared (800nm) Ti:Sapphire laser (Spectra Physics Inc., USA) integrated into an Exitech M2000F Laser Micromachining Workstation (Exitech Ltd, UK) was used. This laser configuration produced 120fs laser pulses with a beam power density of up to 1.25Wcm^{-2}. Beam delivery components allowed the computer control of beam power density and focusing. Typically the beam was focused to a 20µm spot delivering power densities up to 0.1MWcm^{-2}. The ability to deliver such a high power density in such a short period of time allows femtosecond lasers to machine virtually any material to high accuracy. Additionally, since the pulse duration is much shorter than the time required to conduct heat away from the exposed areas, all the absorbed beam energy is translated to an ionization-based ablation process. The laser micromachining was carried out using a direct writing process [4] which makes use of a laser beam tightly focused to a small spot which is moved over the surface of the sample workpiece during machining. The beam fluence at focus is above the ablation threshold of the workpiece material causing machining over the path taken by the beam. Control of beam movement allows arbitrary 2D patterns to be machined and, by overlaying consecutive machining runs with slightly different beam paths, 3D structures can also be produced.

The base substrate for the biochip was a 50mm x 75mm glass plate 1mm thick. 1mm diameter fluid inlet and outlet holes were drilled through the plate using a femtosecond laser adopting a trepanning-based technique to machine a trench around the circumference of the hole. The complete hole is formed when the trench depth extends all the way through the glass sheet and the unmachined central portion of the hole is able to fall away. Hole machining was achieved using a beam power density of 30kW cm^{-2} and an effective workpiece velocity of 0.22mm min^{-1}. The microfluidic channel system, including the containment chamber, were fabricated in a single, adhesive backed, 250µm thick polymer sheet (Melinex A, Katco Ltd. UK) [4]. The benefits of femtosecond laser machining are an extremely high cut quality with no significant machining debris. The lack of debris is of benefit when micromachining composite materials such as the adhesive backed polymer used to form the containment chambers. The sheet comprised of a 250µm rigid polymer sheet coated on both sides with a 50µm thick layer of adhesive which, in turn, was coated with a protective cover. Fluidic channels with containment chambers were machined in a single operation using a beam power

density of 30kW cm^{-2} and an effective workpiece velocity of 5mm min^{-1}. The ionizing nature of the ablation process meant that all three materials of the polymer sheet had similar ablation characteristics. Device assembly was carried out by first removing one layer of protective cover and bonding the polymer to the glass substrate using pressure from a series of heated rollers at 80°C to ensure good contact between the two surfaces. Next the second protective cover was removed and a second, encapsulating, glass plate was bonded to the upper surface. Finally, the completed device was passed through the heated rollers to ensure a firm bond between all layers of the device.

Microelectrodes used for containment chamber fluid conductivity measurement and the generation of electrokinetic forces were fabricated on the lower glass substrate. The substrate was coated with a 100nm gold film with a 5nm chrome adhesion layer using thermal evaporation. Electrode patterns were formed by mask exposure using an EVG 620 mask aligner (EVG, Germany) and a direct laser written (Heidelberg Instruments DWL66, Heidelberg Instruments, Germany) chrome on glass mask followed by wet etching. For devices containing microelectrodes, the polymer fluidic layer and substrate were assembled using the mask aligner to ensure correct positioning of the electrodes relative to the containment chamber.

RESULTS AND DISCUSSION

A fabricated containment chamber held in the microfluidic platform is shown in close-up in figure 6. The opening in the upper plate of the platform is clearly visible over the containment chamber structure. The fluid-driving media channel can be seen traveling horizontally across the image. The control channel extends from the central containment chamber to the right side of the image. Figure 7 shows a normalized conductance measurement from a microelectrode array fabricated on the bottom surface of the containment chamber. The conductance was measured by using a Hewlett Packard 4192A Impedance Analyzer using a 1Vpp, 100kHz, sinusoidal measurement signal. The form of figure 7 is similar to the simulation results of figure 5. Differences between the simulation and measured data can be attributed to differences in the structure of the fabricated chamber which may subtly alter the fluid flow but which were not included in the generalized model. Additionally, even though a relatively high measurement frequency was uses, electrode polarization effects associated with the use of microelectrodes will also influence the conductance measurement. Such factors, associated with the electrical conductance and capacitance of the electrical double layer at the electrode surface, can generally be calibrated for when media of a defined composition is used. The final conductance measured by the electrodes is equivalent to a medium conductivity of around 150µS cm^{-1}.

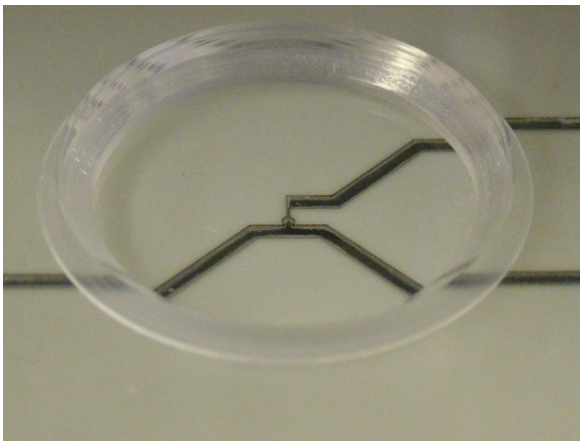

Fig. 6 A close-up view of the fabricated containment chamber held in the fluidic platform

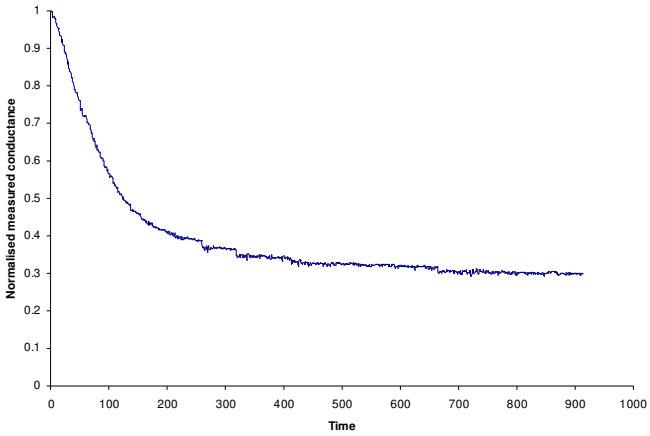

Fig. 7 The change in conductance measured by microelectrodes placed on the lower surface of the containment chamber. The graph shows normalised conductance from measurement of a starting chamber conductivity of 500µS cm^{-1}.

Figure 8 shows images of a containment chamber used to investigate the influence of medium conductivity on the dielectrophoretic characteristics of yeast cells. Dielectrophoresis is the motion of particles induced by exposure to non-uniform electric fields [5,6]. The magnitude and direction of the force is a function of the difference in the electrical conductivity and permittivity of the cell and its suspending medium along with the electric field magnitude, frequency and geometry. In general, for biological cells, at frequencies below 1MHz the dielectrophoretic force is controlled by the difference in medium and cell conductivities whereas permittivity differences tend to dominate above this frequency [7]. If the medium is more conductive than the cell, the cell experiences a negative dielectorphoretic force directed away from areas of high field intensity. In the case of the horizontal interdigitated electrodes shown in figure 8 a negative force would push cells away from the electrode surfaces into the bulk solution above the electrodes. If the medium conductivity is lower than that of the cell a positive force is experienced causing cells to move and collect at the edges of the electrodes where the field intensity is greatest.

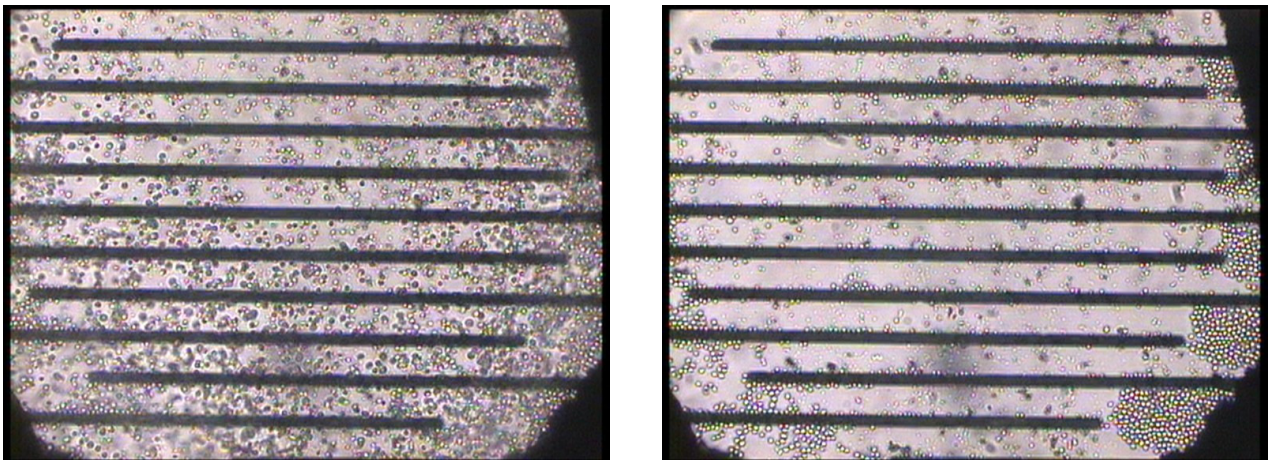

A B

Fig. 8 Images illustrating the influence of suspending media conductivity on the dielectrophoretic collection of yeast cells. (A) Initial conditions with cells in a high conductivity media. Negative dielectrophoresis repells cells from the electrodes into the bulk media. (B) Cells collected at electrode edges by positive dielectrophoresis as the containment chamber media conductivity is reduced by diffusion and forced convection processes.

Figure 8a shows a view of the containment chamber shortly after fluid circulation has commenced. The majority of the cells are in suspension. However, a number have settled onto the lower surface of the chamber. The electrodes were energized with the measurement signal from the Hewlett Packard Impedance Analyzer to allow simultaneous measurement of the chamber conductivity and the generation of a weak non-uniform electric field. The starting conductivity of the chamber fluid is 50mS cm^{-1}, a conductivity high enough to ensure that cells experience a weak negative dielectrophoretic force away from the electrode edges. Figure 8b shows a view of the chamber after 1.5min of operation. After this time the conductivity of the chamber medium has reduced to a value below the conductivity of the yeast cells and so they experienced a positive dielectrophoretic force towards the electrodes. In figure 8b cells can be seen collected as either single cells or clusters along the electrode edges. Additionally, large clusters of collected cells can be observed in the inter-electrode regions around the perimeter of the chamber. These clusters are a result of cell to cell dielectrophoretic collection caused by cells locally distorting the electric field to form local areas of higher field intensity which, in turn, causes cells to form long chains in inter-electrodes regions. As cell concentrations increase the chains become clusters of collected cells. The location of the clusters around the perimeter of the chamber is due to two factors. Firstly cells are pulled to the high field intensity that exists at the tip of alternate interdigitated electrodes. Secondly, the collection process involves the balancing of the dielectrophoretic force with the fluid motion forces. Since the fluid velocity is lower at the perimeter of the chamber, cells in this region will collect more easily than cells in the centre of the chamber. Also, as cells in the center of the containment chamber, pulled by the positive dielectrophoretic force, move closer to the electrodes, the fluid velocity reduces and there is the possibility that the stronger dielectrophoretic force from the end of the electrodes is able to draw cells towards the perimeter of the chamber.

CONCLUSIONS

The optical biochip structures described here have demonstrated the ability to contain suspension cells within defined regions of microfluidic systems by the use of vortex-based circulating fluid movement. Through diffusion and forced convection processes, such structures can also be used to accurately control the physical and chemical environment that restrained cells experience and hence be used to monitor environmental influences on the physico-chemical characteristics of cells. Here, changing the medium ionic concentration and hence electrical conductivity of the containment structure environment has been used to demonstrate the sensitivity of the dielectrophoretic motion of yeast cells to medium conductivity.

ACKNOWLEDGEMENTS

This work has been supported by the Optical Biochip Consortium and funded by the UK research councils (EPSRC Award GR/S23483/01)

REFERENCES

1. Yung-Chiang, C., Yuh-Lih, H. Chun-Ping, J., Ming-Chang, L. and Yu-Cheng, L. (2004) Design of passive mixers utilizing microfluidic self circulation in the mixing chamber. *Lab on a Chip* **4**, 70-77
2. Gower, M.C. (2000) Excimer laser microfabrication and micromachining. *Proc SPIE* **4088** 124-131
3. Rumsby, P.T. (2002) Advanced laser tools for display device production on super large substrates *IMID 2002 Dig*
4. Burt, J.P.H., Goater, A.D., Menachery, A. Pethig, R. and Rizvi, N.H. (2007) Development of microtitre plates for electrokinetic assays. *J. Micromech. Microeng.* **17** 250-257
5. Morgan H., and Green N. (2001) *AC Electrokinetics: Colloids and Nanoparticles, Research Studies Press UK*
6. Pethig R. (2006) Cell physiometry tools based on dielectrophoresis. *BioMEMS and Biomedical Nanotechnology vol 2 ed. M Ferrari Springer, New York*
7. Price, J.A.R., Burt, J.P.H. and Pethig R. (1988) Applications of a new optical technique for measuring the dielectrophoretic behaviour of microorganisms. *Biochim. Biophys. Acta* **964** 221-230